

Lecture Notes in Chemistry 92

Giacomo Bergamini
Serena Silvi *Editors*

Applied Photochemistry

When Light Meets Molecules

 Springer

Lecture Notes in Chemistry

Volume 92

Series editors

Barry Carpenter, Cardiff, UK

Paola Ceroni, Bologna, Italy

Barbara Kirchner, Leipzig, Germany

Katharina Landfester, Mainz, Germany

Jerzy Leszczynski, Jackson, USA

Tien-Yau Luh, Taipei, Taiwan

Claudia Mahlke, Berlin, Germany

Nicolas C. Polfer, Gainesville, USA

Reiner Salzer, Dresden, Germany

The Lecture Notes in Chemistry

The series Lecture Notes in Chemistry (LNC), reports new developments in chemistry and molecular science-quickly and informally, but with a high quality and the explicit aim to summarize and communicate current knowledge for teaching and training purposes. Books published in this series are conceived as bridging material between advanced graduate textbooks and the forefront of research. They will serve the following purposes:

- provide an accessible introduction to the field to postgraduate students and nonspecialist researchers from related areas,
- provide a source of advanced teaching material for specialized seminars, courses and schools, and
- be readily accessible in print and online.

The series covers all established fields of chemistry such as analytical chemistry, organic chemistry, inorganic chemistry, physical chemistry including electrochemistry, theoretical and computational chemistry, industrial chemistry, and catalysis. It is also a particularly suitable forum for volumes addressing the interfaces of chemistry with other disciplines, such as biology, medicine, physics, engineering, materials science including polymer and nanoscience, or earth and environmental science.

Both authored and edited volumes will be considered for publication. Edited volumes should however consist of a very limited number of contributions only. Proceedings will not be considered for LNC.

The year 2010 marks the relaunch of LNC.

More information about this series at <http://www.springer.com/series/632>

Giacomo Bergamini • Serena Silvi
Editors

Applied Photochemistry

When Light Meets Molecules

 Springer

Editors

Giacomo Bergamini
Dipartimento di Chimica
“Giacomo Ciamician”
Università di Bologna
Bologna, Italy

Serena Silvi
Dipartimento di Chimica
“Giacomo Ciamician”
Università di Bologna
Bologna, Italy

ISSN 0342-4901

Lecture Notes in Chemistry

ISBN 978-3-319-31669-7

DOI 10.1007/978-3-319-31671-0

ISSN 2192-6603 (electronic)

ISBN 978-3-319-31671-0 (eBook)

Library of Congress Control Number: 2016947420

© Springer International Publishing Switzerland 2016

This work is subject to copyright. All rights are reserved by the Publisher, whether the whole or part of the material is concerned, specifically the rights of translation, reprinting, reuse of illustrations, recitation, broadcasting, reproduction on microfilms or in any other physical way, and transmission or information storage and retrieval, electronic adaptation, computer software, or by similar or dissimilar methodology now known or hereafter developed.

The use of general descriptive names, registered names, trademarks, service marks, etc. in this publication does not imply, even in the absence of a specific statement, that such names are exempt from the relevant protective laws and regulations and therefore free for general use.

The publisher, the authors and the editors are safe to assume that the advice and information in this book are believed to be true and accurate at the date of publication. Neither the publisher nor the authors or the editors give a warranty, express or implied, with respect to the material contained herein or for any errors or omissions that may have been made.

Printed on acid-free paper

This Springer imprint is published by Springer Nature
The registered company is Springer International Publishing AG Switzerland

Contents

1	Supramolecular Artificial Photosynthesis	1
	Mirco Natali and Franco Scandola	
2	Solar Energy Conversion in Photoelectrochemical Systems	67
	Stefano Caramori, Federico Ronconi, Roberto Argazzi, Stefano Carli, Rita Boaretto, Eva Busatto, and Carlo Alberto Bignozzi	
3	Organic Light-Emitting Diodes (OLEDs): Working Principles and Device Technology	145
	Umberto Giovanella, Mariacecilia Pasini, and Chiara Botta	
4	Light-Emitting Electrochemical Cells	197
	Chia-Yu Cheng and Hai-Ching Su	
5	Industrial Photochromism	227
	Andrew D. Towns	
6	Application of Visible and Solar Light in Organic Synthesis	281
	Davide Ravelli, Stefano Protti, and Maurizio Fagnoni	
7	Photochemical Reactions in Sunlit Surface Waters	343
	Davide Vione	
8	Photodynamic Therapy	377
	Barbara Krammer and Thomas Verwanger	
9	Polymer Nanoparticles for Cancer Photodynamic Therapy Combined with Nitric Oxide Photorelease and Chemotherapy	397
	Fabiana Quaglia and Salvatore Sortino	

10 Chemiluminescence in Biomedicine	427
Mara Mirasoli, Massimo Guardigli, and Aldo Roda	
11 Solar Filters: A Strategy of Photoprotection	459
Susana Encinas Perea	
12 Luminescent Chemosensors: From Molecules to Nanostructures	479
Nelsi Zaccheroni, Francesco Palomba, and Enrico Rampazzo	
13 Photochemistry for Cultural Heritage	499
Maria João Melo, Joana Lia Ferreira, António Jorge Parola, and João Sérgio Seixas de Melo	
Index	531

Chapter 1

Supramolecular Artificial Photosynthesis

Mirco Natali and Franco Scandola

Abstract The conversion of light energy into chemical fuels by artificial means is a challenging goal of modern science, of great potential impact on long-term energy and environmental problems. As such, Artificial Photosynthesis is one of the most active research areas in applied photochemistry. In this tutorial review the basic ingredients of a biomimetic, supramolecular approach to Artificial Photosynthesis are outlined. First, a brief summary of the relevant structural-functional aspects of natural photosynthesis is provided, as a guide to plausible artificial architectures. Then, candidate energy converting reactions are examined, focusing attention on water splitting. The main functional units of an artificial photosynthetic system are dealt with in some detail, namely, charge separation systems, light harvesting antenna systems, water oxidation catalysts, and hydrogen evolving catalysts. For each type of system, design principles and mechanistic aspects are highlighted with specifically selected examples. Some attempts at integrating the various units into light-to-fuels converting devices are finally discussed. Throughout the review, the emphasis is on systems of molecular and supramolecular nature.

1.1 Introduction

Boosted by the rapid economic development of a growing world population, the global energy demand (now about 15 TW) is expected to double by 2050 and to triple by 2100. How to satisfy this enormous energy demand is the most pressing challenge facing society today. The main present energy source, fossil fuels, cannot be considered as a viable solution, not only for their limited availability, but because atmospheric CO₂ levels (already at more than 50% above the pre-industrial values) cannot increase further without catastrophic consequences

M. Natali (✉) • F. Scandola

Department of Chemical and Pharmaceutical Sciences, University of Ferrara, and Centro Interuniversitario per la Conversione Chimica dell'Energia Solare (SOLARCHEM), sezione di Ferrara, Via Fossato di Mortara 17-19, 44121 Ferrara, Italy
e-mail: mirco.natali@unife.it; snf@unife.it

on climate change. It is clear that any long-term solution to the energy problem relies on the identification and exploitation of alternative energy sources that must be abundant, inexpensive, environmentally clean, and geographically widespread. In terms of such requirements, solar power (120,000 TW average irradiation at earth surface) presents itself as the most promising source of renewable energy available. In Nature, massive utilization of solar energy to sustain biological life is performed by a variety of photosynthetic organisms (plants, algae, cyanobacteria) that have evolved, along ca 2 billion years, to convert CO₂ and water into carbohydrates and oxygen. The development of artificial systems capable of efficiently converting light energy into practical fuels (Artificial Photosynthesis) can thus be envisioned as a research field of great potential, in principle able to provide a definitive solution of our energy problem.

In this tutorial review the basic ingredients of a biomimetic, supramolecular approach to Artificial Photosynthesis are outlined. First, a brief summary is given of the relevant structural-functional aspects of natural photosynthesis, both anoxygenic (Sect. 1.2.1) and oxygenic (Sect. 1.2.2). Then, candidate energy converting reactions are examined, focusing attention on water splitting (Sect. 1.3.1). The main functional units of artificial photosynthetic systems are dealt with in some detail, namely charge separation systems (Sect. 1.3.2), light harvesting antenna systems (Sect. 1.3.3), water oxidation catalysts (Sect. 1.3.4), and hydrogen evolving catalysts (Sect. 1.3.5). Some attempts at integrating the various units into light-to-fuels converting devices are finally discussed (Sect. 1.3.6). Throughout the review, the emphasis is on systems of molecular and supramolecular nature. In the discussion of the various topics, rather than aiming at comprehensive literature coverage, we have attempted to highlight design principles and mechanistic aspects with specifically selected examples.

1.2 Natural Photosynthesis

In Nature, photosynthesis, i.e., the conversion of light energy into chemical energy, is performed by a variety of organisms, ranging from plants to bacteria. The simplest form of photosynthesis is probably that performed by non-sulfur purple bacteria, such as *Rhodobacter sphaeroides* and *Rhodospseudomonas viridis*, where light energy is simply used to perform photophosphorylation, i.e., the conversion of adenosine diphosphate (ADP) into adenosine triphosphate (ATP), the molecular “energy currency” of the cell. At the other extreme of complexity is the oxygenic photosynthesis, performed by cyanobacteria, algae, and higher plants, whereby light energy is used to power the conversion of water and carbon dioxide into oxygen and sugars. A detailed description of the vast field of natural photosynthesis [1] is clearly outside of the scope of this tutorial review. A brief outline of the main features of the bacterial and oxygenic photosynthetic apparatuses will be given here, however, as these systems represent a powerful source of inspiration for research on artificial photosynthesis.

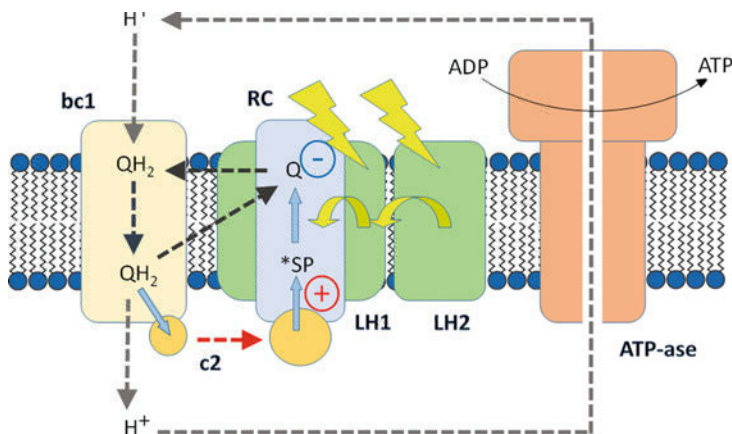


Fig. 1.1 Schematic representation of the relevant subunits involved in bacterial photosynthesis: the reaction center (RC), the LH1 and LH2 antenna systems, the bc1 complex, a small mobile cytochrome c2, and the ATP-ase enzyme

1.2.1 Bacterial

A schematic block-diagram picture of a bacterial photosynthetic membrane is shown in Fig. 1.1.

In simple terms, the overall function of this device is as follows: The light energy is primarily captured by light harvesting (“antenna”) units, i.e., pigment protein complexes containing a large density of chromophoric molecules. Two types of such antenna units are usually present in the membrane, smaller LH2 units and the larger LH1 unit directly surrounding the reaction center. The energy is rapidly channeled, by means of exciton diffusion within and energy transfer between the antenna units to the reaction center, where a “special pair” of bacteriochlorophylls (SP) is excited. This triggers in the reaction center a series of electron transfer steps that lead to separate a positive and negative charge across the width of the membrane, the electron being localized on a quinone and the hole at the special pair. The reduced quinone picks up protons from the aqueous cytoplasmic phase, diffuses within the membrane to the cytochrome bc1 complex, where it is eventually reoxidized by the mobile cytochrome c2, releasing protons in the periplasmic aqueous phase. The cytochrome c2 shuttles from bc1 to RC giving back the electrons, thus closing the photoinduced electron transfer cycle. The net effect, therefore, is simply the building-up of a proton concentration gradient across the membrane. This proton electromotive force is then used by the ATP-ase enzyme for phosphorylation of ADP to ATP. The overall process is thus that of a cyclic photophosphorylation (Eq. 1.1, where P is inorganic phosphate)



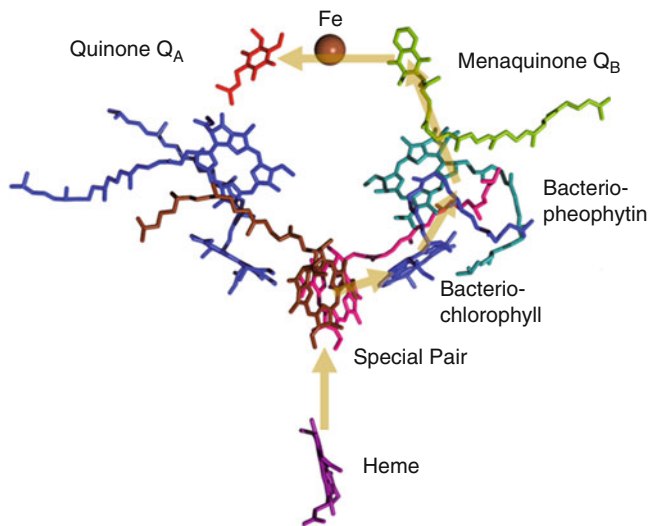


Fig. 1.2 Spatial arrangement of the cofactors within the protein matrix (not shown) of the reaction center of *Rhodospseudomonas viridis*. They are arranged in two quasi-symmetrical branches consisting of “special pair” of bacteriochlorophylls, bacteriochlorophyll, bacteriopheophytin, and quinone. A heme group of the four-heme reaction center cytochrome is also shown. The arrows point out the electron transfer chain that leads to charge separation following excitation of the special pair

In recent years, great progress has been achieved in the characterization by diffraction methods of the various functional subunits of the bacterial photosynthetic membranes, shining light on important aspects of the structure-function relationship. For their relevance to the biomimetic approach outlined in subsequent sections, attention is focused here on the structures and function of reaction center and on the antenna units. A milestone in the field, awarded with the Nobel Prize in Chemistry 1988, has been the determination of the structure of the reaction center of *Rhodospseudomonas viridis* by Dessenhofer, Huber, and Michel [2]. The spatial arrangement of the relevant cofactors, as shown in Fig. 1.2, is crucial to the function of the RC as a photoinduced charge separating device. Following selective excitation (see later) of the special pair of bacteriochlorophylls, a sequence of electron transfer steps takes place along one of the two branches of cofactors: [3] to accessory bacteriochlorophyll (3 ps), to bacteriopheophytin (1 ps), to menaquinone Q_A (150 ps), to quinone Q_B (200 ps). The hole on the special pair is eventually scavenged by electron transfer from the reduced reaction center cytochrome (0.3 ps). The long-range charge separation so obtained (22.4 Å from special pair to Q_A) is highly efficient (98 %) and long-lived (milliseconds). The key to such a performance lies in the multi-step nature of the process, where all the forward steps are kinetically optimized relative to the potentially detrimental back electron transfer steps (for a discussion of the factors that determine electron transfer kinetics, see later, Sect. 1.3.2).

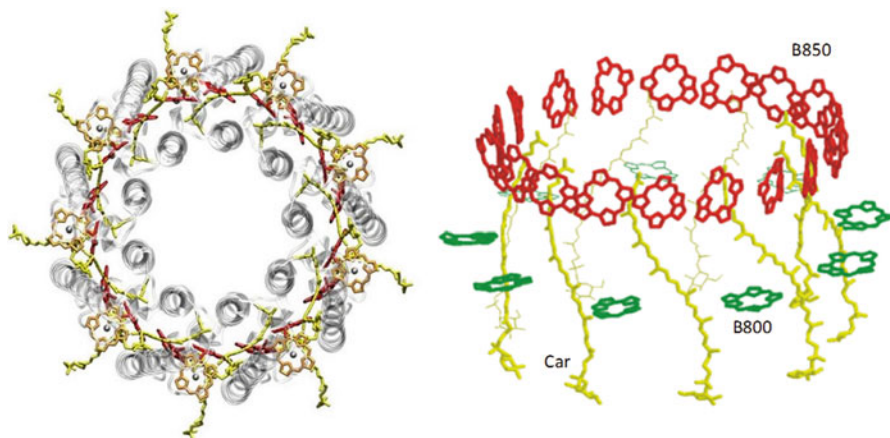


Fig. 1.3 Structure of the LH2 antenna unit of *Rhodospseudomonas acidophila*. *Left*: azimuthal view (perpendicular to membrane plane) showing the circular nonameric double-pillared protein structure. *Right* lateral view after deletion of the protein structure, showing the arrangement of three different types of chromophores: bacteriochlorophylls (B800), bacteriochlorophylls (B850), and carotenoids (Car)

Excitation of the reaction center takes place only in negligible amounts by direct light absorption. In fact, the light incident on the photosynthetic membrane is almost totally absorbed by the chromophores in the antenna units. Detailed structural and spectroscopic studies have provided clear pictures of the function of these units. The structure of the LH2 type of antenna, isolated from *Rhodospseudomonas acidophila*, [4] is shown in Fig. 1.3. In LH2, a circular double-pillared structure, made of nine heterodimers of α - and β -apoproteins spanning the membrane, acts as container of a dense ensemble of chromophores: 27 bacteriochlorophylls and 9 carotenoids. The bacteriochlorophylls are of two types, differing in wavelength of maximum absorption and position: 9 B800 molecules, lying parallel to the membrane surface, forming a ring on the cytoplasmic side; 18 B850 molecules form a tightly coupled perpendicular ring with slipped cofacial arrangement near the periplasmic side of the complex. The carotenoids, with strong visible absorption, have an extended all-trans conformation and span the entire depth of the complex, coming into van der Waals contact with both groups of BChls. Upon light absorption by the LH2 complex, a series of ultrafast energy transfer processes takes place: Car to B800–850 (140 fs), [5] B800 to B850 (0.9 ps), within the B850 ring (50–100 fs) [6]. Due to the strong interchromophore coupling, excitation in the B850 ring is partially delocalized, with an exciton delocalization length of ca four bacteriochlorophyll units [7].

The LH1 antenna units bear some structural similarity to the LH2 ones, being again based on a double-pillared cyclic protein structure, holding a large number of chromophores. The dimensions of the LH1 ring are larger, however, being composed of 16–15 heterodimers depending on the bacterium. Each heterodimer holds a pair of bacteriochlorophyll molecules, forming again a large, tightly coupled ring

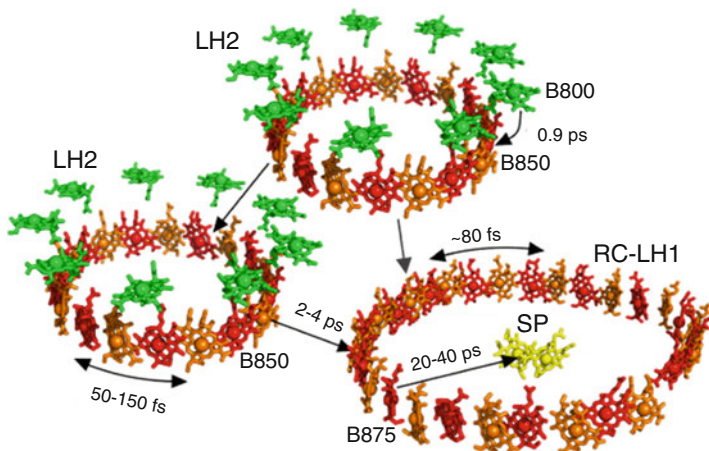


Fig. 1.4 Schematic of the processes conveying light excitation energy from the LH2 and LH1 antenna systems to the special pair of the reaction center of bacterial photosynthesis

with slipped cofacial arrangement, with maximum absorption at 875 nm. The dimensions of LH1 are appropriate to host the reaction center in its central cavity, and indeed a number of structures of LH1-reaction center complex are now available [8]. In such structures, the B875 ring of LH1 and the special-pair bacteriochlorophylls of RC are aligned on the same level in the transmembrane region, in an optimal arrangement for selective excitation of the special pair by energy transfer from LH1. In the bacterial photosynthetic membrane, LH2 units and LH1-RC complexes are assembled in densely packed arrays, [9] where efficient energy transduction takes place. A summary of the time resolved energy transfer processes [6, 7] taking place in the bacterial photosynthetic membrane is given in Fig. 1.4.

In summary, the bacterial photosynthetic membrane is a perfect device performing the following light-induced functions: (a) efficient light energy harvesting, (b) fast and efficient transfer of the excitation energy to the reaction center, (c) efficient, long-lived trans-membrane charge separation. The dark processes that convert this charge separation into trans-membrane proton gradient and ultimately lead to generation of ATP fuel are of course extremely important from the biological viewpoint, but less interesting in the context of possible extensions to artificial photosynthesis.

1.2.2 Oxygenic

Unlike bacterial photosynthesis, which is a cyclic (photophosphorylation) process, the photosynthesis carried out by higher plants, algae, and cyanobacteria is characterized by a net chemical reaction consisting in the splitting of water into

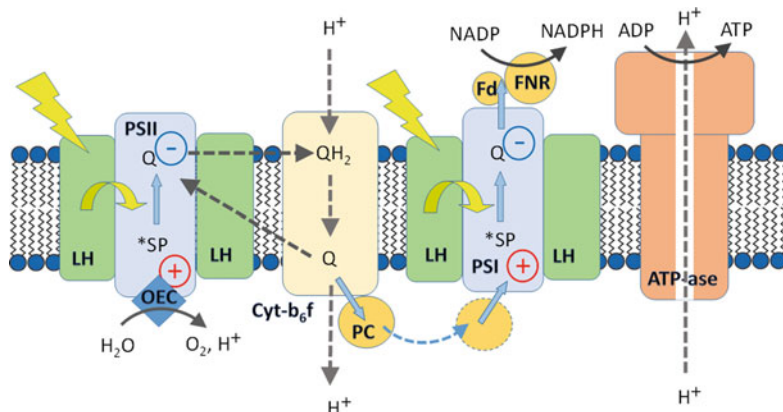


Fig. 1.5 Schematic diagram of the main functional subunits of an oxygenic photosynthetic membrane (for details, see text)

molecular oxygen, protons and electrons. The protons are used, as in bacterial photosynthesis, for the ATP synthesis and the electrons for the reduction of carbon dioxide to carbohydrates. Thus, the net reaction is shown in Eq. 1.2.



A schematic block diagram of an oxygenic photosynthetic membrane is given in Fig. 1.5. A number of subunits are similar, at least from a functional viewpoint, to those of bacterial photosynthesis, e.g., reaction centers for charge separation (here called “photosystems, PS”), light harvesting antenna systems, ATP-ase. The main difference, however, lies in the intrinsic two-photon architecture of the process that requires the operation of two charge separating reaction centers, photosystems I and II. If we focus on the left part of Fig. 1.5, starting from photon absorption by the antenna (LH), energy transduction to the reaction center (PSII), charge separation in PSII, diffusion of reduced quinone with proton uptake on the stroma side and discharge on the lumen side mediated by the cytochrome b6f complex (Cyt-b6f), all these processes bear a clear resemblance to those of bacterial photosynthesis. But now, rather than being short-circuited (as in the bacterial case) on the original reaction center, the electron transfer chain goes on, by means of a diffusing plastocyanin (PC), to the next reaction center, PSI, where a second photoinduced charge separation process takes place. The overall function is that of a device where two photosystems are chemically connected “in series”. The oxidation potential of the “positive” end of PSII is used, with the help of a specific oxygen evolving catalyst (OEC, *vide infra*), for the oxidation of water on the periplasmic side, and the reducing power at the “negative” end of PSI is used, with the intervention of ferredoxin (Fd) and ferredoxin-NADP⁽⁺⁾ reductase (FNR), for the reduction of NADP⁺ to NADPH. The primary reduced product NADPH, together with the ATP generated as usual taking advantage of the proton electromotive force, is

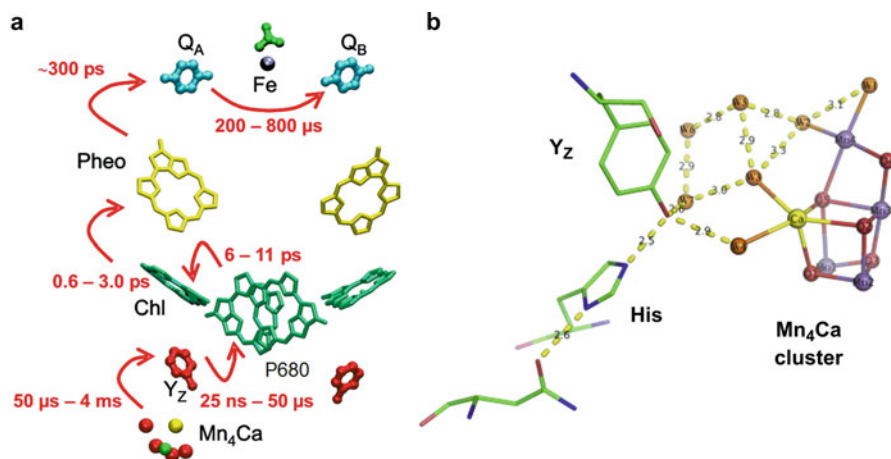


Fig. 1.6 (a) Arrangement of cofactors and electron transfer chain in Photosystem II (adapted with permission from ref. 10, copyright © 2012 Elsevier). (b) Detailed view of the OEC (adapted with permission from ref. 15c, copyright © 2011 Elsevier), showing the Mn₄Ca cluster, the primary electron acceptor tyrosine Y_Z and the nearby histidine, and the hydrogen-bond network of water molecules

used downstream in a complex thermal cycle (Calvin cycle) for CO₂ fixation and carbohydrate synthesis. Any detailed description of structure and function of the subunits of such a complex system is clearly outside the scope of this review. Let us simply point out a few aspects that may be relevant to the discussion in the subsequent sections.

Despite the wide differences in their organisms and functions, the charge separation devices involved in all oxygenic and anoxygenic (bacterial) photosynthetic systems are remarkably similar. A picture of the cofactors of PSII from *Thermosynechococcus elongatus* is shown in Fig. 1.6 [10].

Aside from the presence of chlorophylls rather than bacteriochlorophylls, the similarity to the structure of the bacterial reaction center of Fig. 1.2 is evident, with the two-branched structure involving special pair (P680), monomeric chlorophyll, pheophytin, and quinone. The photoinduced electron transfer sequence from special pair to quinones is again very similar. The main difference lies in the “positive” end of the chain, where in this case the hole on the special pair is filled with electrons coming, with a tyrosine residue (Y_Z) acting as a relay, from the Mn₄Ca cluster (Oxygen Evolving Complex, OEC) that is the actual catalyst for water oxidation. The ability of the OEC to perform such a complex process (four-electron oxidation of two water molecules, formation of a new O-O bond, and release of four protons) relies on its very specific structure, revealed by a recent high-resolution X-ray structure [15b]. Figure 1.6b shows the chair-like shape of the OEC, with the distorted cubane structure including three Mn, one Ca, and four bridging oxygen atoms, and the isolated fourth Mn and one bridging oxygen atom. It also shows four water molecules directly coordinated to the metal centers and other water molecules

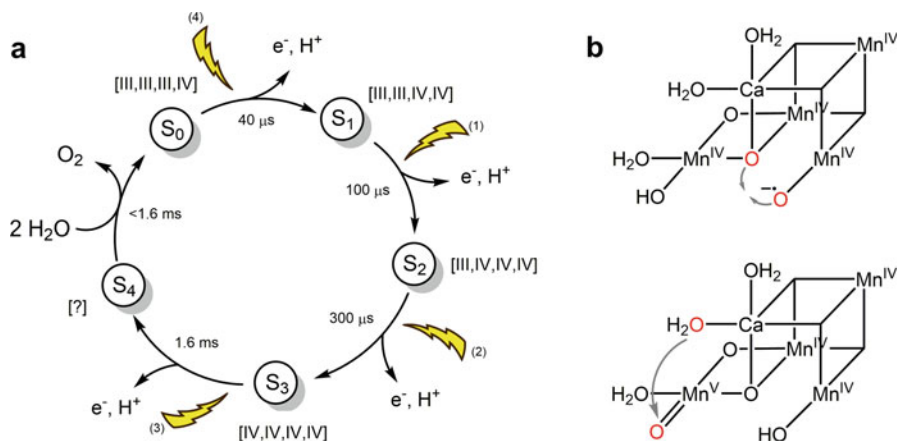


Fig. 1.7 (a) Kok cycle of photosynthetic water oxidation. Starting from the dark-stable S_1 state, photon absorption causes sequential electron abstraction from the OEC, accompanied by charge-compensating deprotonation steps. Oxidation-state combinations of the Mn ions are shown for the various S_0 - S_3 states. Typical time constants of the ET steps are also indicated [12]. (b) Two plausible structures of the S_4 state, with corresponding mechanisms of O-O bond formation: oxyl radical coupling (*upper*) or water nucleophilic attack (*lower*) [13]

participating to a hydrogen-bond network linking the Mn_4Ca -cluster and Y_Z , and further from Y_Z to a nearby histidine.

The stepwise oxidation of the OEC by sequential photoinduced electron abstraction is described by the Kok cycle, [11] where four oxidation states of the OEC are termed S_i ($i = 0-4$), S_0 being the most reduced state and S_4 the most oxidized state in the catalytic cycle (Fig. 1.7a).

As shown by the flash number dependent oscillating pattern in O_2 evolution, the dark-stable state is S_1 . From there, three photons are needed to effect the $S_1 \rightarrow S_2$, $S_2 \rightarrow S_3$, and $S_3 \rightarrow S_0$ transitions. In the last transition, likely with the intervention of an S_4 state as an intermediate, oxygen is evolved. Then, a fourth photon is needed to regenerate the dark-stable state S_1 . As to the oxidation states of the four Mn centers of the OEC in the various S_i states, there is a general agreement that the dark-stable S_1 state of the OEC has two Mn(III) and two Mn(IV) centers. The oxidation states of the S_0 , S_2 , and S_3 states can be inferred by one-electron reduction or oxidation steps. The detailed nature of the elusive S_4 state, where oxygen evolution takes place is unknown. Among several hypotheses, [12] two plausible ones are (a) an all-Mn(IV) structure with a coordinated oxyl radical or (b) a structure with three Mn(IV) and one Mn(V)-oxo group. These two structures are related to two plausible mechanisms for O-O-bond formation (Fig. 1.7b): (a) oxyl radical coupling, (b) water nucleophilic attack [13]. A point worth of mention is that in the successive steps of the Kok cycle the OEC accumulates four oxidizing equivalents delivered by the Y_Z radical, an oxidant with an approximately constant potential (close to +1.1 V). This would be unfeasible without a charge-

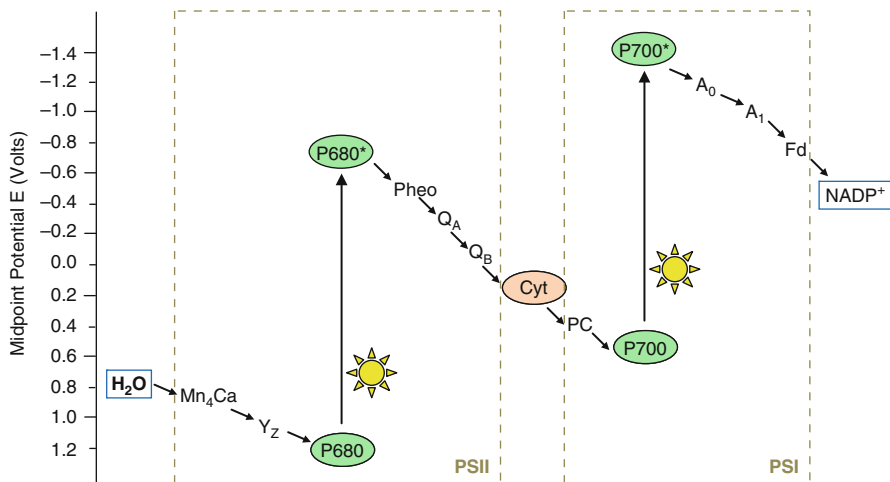


Fig. 1.8 Z-scheme of the energetics of oxygenic photosynthesis, pointing out the relationships between absorbed photon energy, chemically converted energy, and energy price paid for charge separation

compensating mechanism, by which protons are removed from acid-base sites of the OEC and relocated towards the aqueous phase.

As to the portion of the photosynthetic mechanism taking part downstream of PSII, without going into any detail, let us just point out that the structure and function of PSI [14] are again rather similar to those of PSII, with a similar two-branched chain of co-factors, involving special pair (P700), monomer chlorophyll, a second monomer chlorophyll, and quinone, and similar electron transfer chain events. The related cofactors in the two photosystems, however, have different redox properties, as shown in Fig. 1.8, where the chain of electron transfer events taking place along the whole photosynthetic process is depicted on a potential scale. This electrochemical energy diagram (known as Z-scheme) shows clearly the very reason for the use of two photosystems in series by oxygenic photosynthesis. In fact, the potential difference required for water oxidation and NADP reduction (ca 1.2 V) does not exceed the energy of a single photon (ca 2.0 eV). A large amount of the photon energy is lost, however, by each photosystem as driving force for charge separation. Therefore, two photosystems operating in series are actually required.

Although many other aspects of the complex machinery of oxygenic photosynthesis are interesting, let us only mention a few points about the light harvesting antenna systems. First, there are differences in the chromophoric units of the two types of photosyntheses, mainly dictated by the different habitats of the organisms: in plant photosynthesis the main chromophores are chlorophylls, absorbing at shorter wavelengths than their bacterio-analogues. Moreover, with respect to the LH2 and LH1 antennae of bacterial photosynthesis, the antenna units of plant photosynthesis consist of smaller, less symmetric and apparently less highly

ordered subunits [15, 16]. This reflects a difference in function, which in this case requires, for optimal performance, not only efficient energy transfer to the reaction center but also a balance of the excitation pressure on the two photosystems working in series [17]. Since the absorption spectra of PSI and PSII are different, variations in light quality may drive both photosystems to a different extent, leading to imbalances. In such a case, a process called “state transition”, regulated in a complex manner by phosphorylation, [18] redistributes the amount of excitations between PSI and PSII. In practice, a mobile pool of antenna complexes (LHCII) is able to reversibly associate with PSI or PSII, depending on which is preferably excited.

1.3 Artificial Photosynthesis

1.3.1 Functional Units and Candidate Reactions

With the general term “Artificial Photosynthesis” a process is commonly defined whereby light energy is exploited for the conversion of suitable substrates into chemicals with high energy content, namely fuels. Inspired by the complex machinery of natural photosynthetic organisms (Sect. 1.2), an artificial system capable of achieving this goal must be composed of several functional units, as shown in Fig. 1.9, which include: (i) an antenna system based on a series of chromophores which are responsible for the light-harvesting and the excitation energy funneling towards the reaction center, (ii) a charge separation system where the excitation energy is converted through a series of photoinduced and thermal electron transfer processes into an electrochemical potential residing in a hole and an electron kept

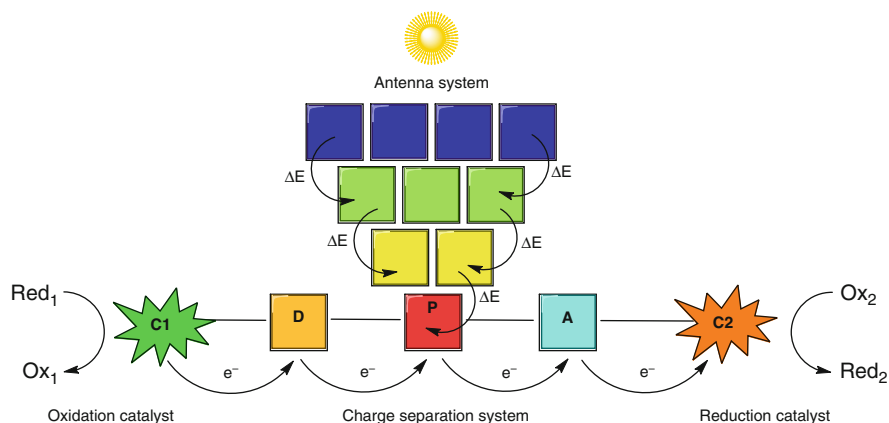
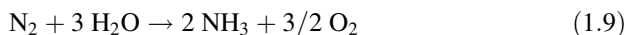
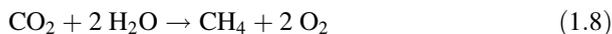
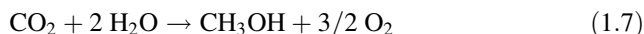
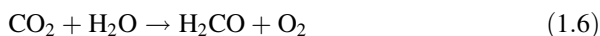
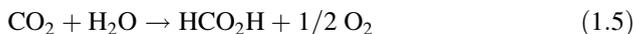


Fig. 1.9 Schematic representation of an artificial photosynthetic system comprising antennae, charge separation, and catalysts. Abbreviations used: *P* photosensitizer, *D* donor, *A* acceptor, *C1* oxidation catalyst, *C2* reduction catalyst, *Red*₁, *Ox*₂ substrates, *Ox*₁, *Red*₂ products

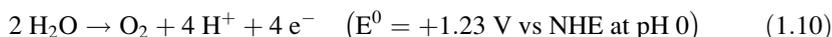
far apart one to each other, and (iii) two catalytic units capable of stepwise collecting and storing electrons and holes from the charge separation system to drive multi-electron redox processes on the substrates at low activation energy.

Several attempts have been performed towards the construction of either charge separation or antenna systems and towards the integration of both functional units into a single molecular device by adopting different molecular design and synthetic strategies. The basic guidelines towards this goal and some of the most relevant results will be outlined in the following sections (Sects. 1.3.2 and 1.3.3 for charge separation systems and antennae, respectively).

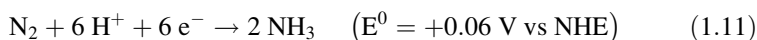
As far as the chemical redox reactions are concerned, several schemes can be in principle drawn for application into an artificial photosynthetic system, all sharing the common feature that the ideal substrates are naturally abundant molecules while the related products should be high energy content chemicals to be exploited either directly (e.g., combustion, fuel cells, etc.) or as intermediates for industrially relevant reaction processes. Some examples include processes such as water splitting (Eq. 1.3), carbon dioxide reduction (Eqs. 1.4, 1.5, 1.6, 1.7, 1.8), and nitrogen reduction (Eq. 1.9).



Notably, all these processes have in common water oxidation to dioxygen (Eq. 1.10) as the anodic half-reaction and a large extent of the energy required to power the overall reactions (Eqs. 1.3, 1.4, 1.5, 1.6, 1.7, 1.8, and 1.9) is deserved to this oxidative step.



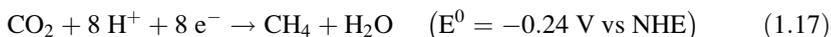
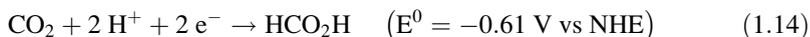
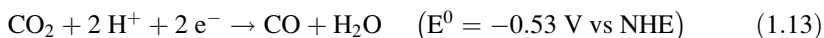
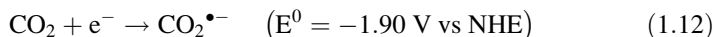
Apart from thermodynamics, this latter reaction is also hampered by important kinetic hurdles, intimately connected to the reaction mechanism which requires the abstraction of four electrons and four protons from two water molecules with the concomitant formation of an oxygen-oxygen bond [19]. As a result, huge amount of studies are aimed at solving this quite complicated issue (see below Sect. 1.3.4).



As regarding the cathodic half-reaction, conversion of nitrogen into ammonia (Eq. 1.11) is a quite demanding process which is accomplished in certain natural

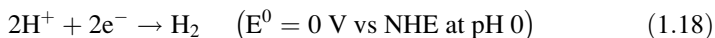
photosynthetic organisms by nitrogenase enzymes. In these natural systems strongly reducing agents are not sufficient to promote the reaction which requires additional energy inputs (e.g., ATP). This is mainly dictated by the high activation barrier of the nitrogen-to-ammonia transformation since the mechanism requires the accumulation of six electrons, the rupture of a triple nitrogen-nitrogen bond, and the contemporary formation of six nitrogen-hydrogen bonds. As a result this chemical reaction is very difficult to afford in an artificial manner and only few examples are indeed reported which, however, perform modestly and under quite harsh reducing conditions [20]. Therefore employing nitrogen reduction as the cathodic reaction in an artificial photosynthetic system is far from a viable solution.

Reduction of carbon dioxide is, on the other hand, a potential cathodic reaction in artificial photosynthesis providing a direct way to the production of liquid fuels in a carbon-neutral fashion. The one-electron reduction of CO_2 (Eq. 1.12) is, however, highly disfavored from a thermodynamic viewpoint whereas the proton-assisted reductions significantly lower the thermodynamic barrier (Eqs. 1.13, 1.14, 1.15, 1.16, and 1.17).



This, however, introduces non-trivial kinetic hurdles since the reduction mechanism has to deal with multi proton-coupled electron-transfer (PCET) steps. Moreover, to manage such proton electron transfer reactions a suitable catalyst must directly bind the CO_2 substrate and, since carbon dioxide is a linear and somewhat inert molecule, this process usually requires additional energetic efforts [21]. Taken together, these intrinsic restrictions significantly affect the results attainable from catalytic CO_2 reduction, usually achieving CO and/or formic acid as the main products, while rarely methanol or methane, and also showing, with few exceptions, [22] poor selectivity and/or parasite reactions such as hydrogen evolution [23].

With respect to both nitrogen and carbon dioxide reduction, proton reduction to dihydrogen (Eq. 1.18)



is a much easier solution. Indeed, although a catalyst is anyway required to enable hydrogen evolution, the overall reaction is less affected by parasite processes and competitive pathways. Moreover, hydrogen is a clean fuel since its combustion in

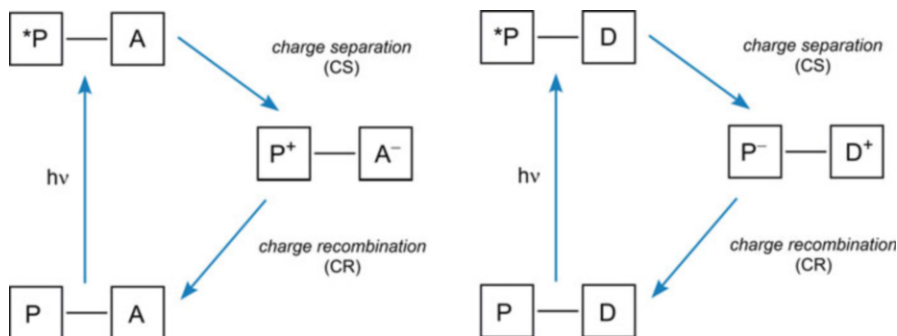


Fig. 1.10 Photoinduced electron transfer processes: oxidative quenching by an acceptor A (*left*) and reductive quenching by a donor D (*right*) of the light-harvesting photosensitizer P

the presence of oxygen produces heat, its combination with oxygen in a fuel cell generates electricity and heat, and the only byproduct of such energy-producing processes is water. More importantly, once hydrogen is produced via water splitting several application can be envisaged in addition to its direct consumption as a fuel. Indeed, it may also be exploited for catalytic hydrogenation of CO_2 to produce formic acid [24] which can be used as a preservative agent or synthetic precursor, or even as a liquid hydrogen storage material. Moreover, hydrogen produced from photochemical water splitting can be used in combination with CO_2 in the presence of suitable bacteria to renewably generate either biomass or liquid fuels such as alcohols [25]. Altogether, these evidences clearly demonstrate the actual potential arising from proton reduction catalysis and thus explain the enormous efforts made in the last years to prepare and characterize artificial systems capable of promoting this reaction (see below Sect. 1.3.5).

1.3.2 Charge Separation Systems

In natural photosynthesis, “reaction centers” (bacteria) and “photosystems” (plants) are the subunits that play the key role of converting the excitation energy, via photoinduced charge separation, into chemically exploitable redox potential. Any conceivable artificial photosynthetic system must include at least one subsystem with this functional role, that can be shortly named “charge separation system”. In its simplest terms, a charge separation system is a supramolecular device where light absorption by a photoexcitable molecular component (photosensitizer, P) is followed by electron transfer to an acceptor A (Fig. 1.10, left) or from a donor D (Fig. 1.10, right), leading to a pair of one-electron oxidized and reduced transient species. As shown later, many variations of this basic scheme can be envisioned, with various degrees of complexity in both supramolecular architecture and electron transfer pathways. A simple two-component (“dyad”) system, such as, e.g., those of Fig. 1.10 can be used, however, to introduce some basic concepts. The key

requisites for a good charge separation system are as follows: the one-electron oxidized and reduced products (i) should be formed in high quantum yield, (ii) should store a large fraction of the original excitation energy in the form of redox potential, and (iii) should be long-lived towards charge recombination. The achievement of such requisites, relying on a complex interplay of kinetic and thermodynamic factors, is not trivial and constitutes the main challenge in the design of artificial charge separation systems.

A general theoretical framework for understanding electron transfer processes in supramolecular systems is provided by the Marcus non-adiabatic classical electron transfer theory, [26, 27] that relates the electron transfer rate constant to a number of relevant parameters (Eq. 1.19).

$$k = \left(\frac{4\pi^3}{h^2 \lambda k_B T} \right)^{\frac{1}{2}} V^2 \exp \left[- \frac{(\Delta G^o + \lambda)^2}{4\lambda k_B T} \right] \quad (1.19)$$

In Eq. 1.19 V is the electronic matrix element, h is Planck's constant, k_B is Boltzmann's constant, T is the temperature, ΔG^o is the standard free energy change of the process, and λ is the so-called reorganization energy, i.e., the energy required to reorganize the nuclear geometry of donor and acceptor as well as their solvation environments upon electron transfer. The reorganization energy has inner (molecular geometry) and outer (solvent) contributions (Eq. 1.20)

$$\lambda = \lambda_i + \lambda_o \quad (1.20)$$

that in classical terms are given as in Eqs. 1.21 and 1.22

$$\lambda_o = e^2 \left(\frac{1}{2r_1} + \frac{1}{2r_2} - \frac{1}{r_{12}} \right) \left(\frac{1}{D_{op}} - \frac{1}{D_s} \right) \quad (1.21)$$

$$\lambda_i = \frac{1}{2} k \Delta Q^2 \quad (1.22)$$

where D_{op} and D_s are the optical and static solvent dielectric constants respectively, r_1 and r_2 are the radii of the two molecular components, r_{12} is the inter-component distance, e is the electron charge, ΔQ represents the nuclear displacement accompanying electron transfer along a relevant nuclear coordinate Q , and k is an appropriate force constant for that motion.

In order to produce the charge separated state with high quantum yield [requisite (i)], the forward electron transfer reaction (charge separation) must be as fast as possible, so as to be able to beat the excited-state lifetime of the sensitizer (which for most organic chromophore singlet states is of the order of few nanoseconds). For the charge separated state surviving long enough to permit utilization of the stored redox power [requisite (iii)], the back electron transfer reaction (charge recombination) must be as slow as possible. A solution to this double constraint is provided by the Marcus theory (Eq. 1.19) whereby, assuming for the sake of simplicity a constant electronic matrix element V , [28, 29] the main source of

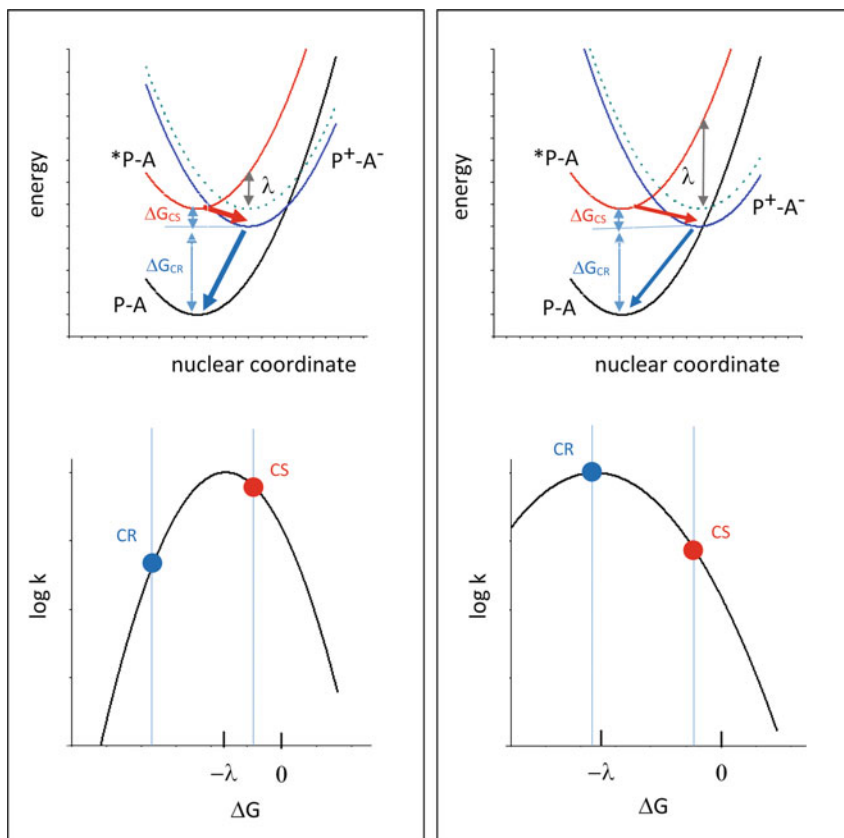


Fig. 1.11 Effects of small (*left panel*) or large (*right panel*) reorganization energy λ on photoinduced charge separation (CS) and recombination (CR). *Upper part*: potential energy curves for ground state (P-A), excited state (*P-A) and charge separated state (P⁺-A⁻) of a photosensitizer-acceptor dyad. *Lower part*: charge separation and recombination rates as predicted by Eq. 1.19

difference between forward and back ET rates is to be looked in their driving forces, ΔG . According to Eq. 1.19, the dependence of $\log k$ on driving force is quadratic, with values first increasing for increasing exergonicity (“normal” region), reaching a maximum value for $-\Delta G = \lambda$ (activationless regime), and then decreasing for more exergonic reactions (Marcus “inverted” region). It is clear that the key rate-determining factor is not the driving force as such, but rather its value relative to the reorganization energy λ . Two hypothetical situations of small and large λ , with the corresponding predictions of Eq. 1.19, are sketched in Fig. 1.11. Clearly, the ideal situation in order to obtain fast charge separation and slow charge recombination is to have, as in Fig. 1.11 (left panel), the first process in the “normal” free energy region (possibly as close as possible to the activationless regime) and the latter as a much more exergonic process lying deep into the “inverted region”. The comparison between left and right panels of Fig. 1.11 clearly shows that having a small λ is

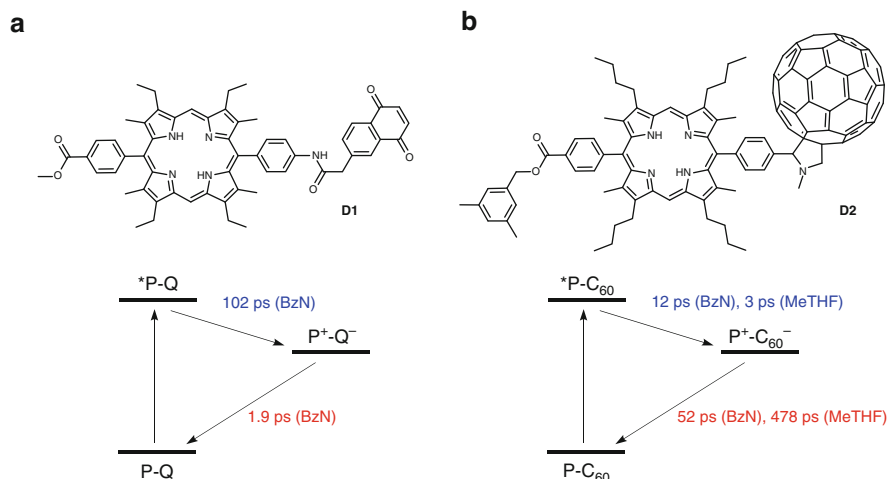


Fig. 1.12 Photoinduced charge separation and recombination in dyads (a) **D1** and (b) **D2** involving a porphyrin as photoexcitable chromophore (P) and a quinone (Q) [30] or a fullerene (C_{60}) [31] as acceptor unit, respectively

instrumental towards the achievement of this ideal kinetic condition. Furthermore, it is obvious that the smaller λ the larger the fraction of the excitation energy that can be converted, in the kinetically optimal situation ($-\Delta G_{CS} = \lambda$), into redox energy of the charge separated products (condition (ii) above).

In the light of the above arguments, the design of artificial charge separation systems should preferably use molecular components that, besides having the appropriate excited-state and redox properties, could warrant small reorganization energy values. Typically, relatively large molecules with highly delocalized electronic systems are expected to induce little solvent repolarization (large r_1 and r_2 in Eq. 1.21) and to undergo small internal geometry changes (small ΔQ in Eq. 1.22) upon ET. As to the environment to be used, a low-polarity solvent (small D_s in Eq. 1.21) will be beneficial to reduce λ_0 . The comparison between the behavior of the two dyads **D1** and **D2** in Fig. 1.12 is instructive in this regard. They are made of the same photosensitizer, a porphyrin, and two different acceptors with similar redox properties, namely, a quinone and a fullerene. Despite the very similar energetics, the two dyads behave (in the same solvent, e.g., benzonitrile) quite differently: in the fullerene-based system **D2** (Fig. 1.12b) fast charge separation is followed by slow charge recombination, but the opposite situation occurs in the quinone-based **D1** (Fig. 1.12a).

This difference can be traced back, at least qualitatively, to differences in reorganization energies: [32] the fullerene A/A^- couple, with its larger dimensions and electronic delocalization, provides a smaller λ than the quinone-based one. A further reduction in λ , and thus a further gain in charge separation vs recombination rates, can be obtained by lowering the solvent polarity, as shown by the comparison between the time constants obtained for dyad **D2** in benzonitrile and in 2-methyltetrahydrofuran. With reference to the schemes of Fig. 1.11, the large- λ situation

(right panel) could be used to describe the porphyrin-quinone dyad, while for the porphyrin-fullerene one (and particularly so in MeTHF) the small- λ situation (left panel) very likely applies.

As discussed above, a clever choice of molecular components and medium, providing the right combination of driving forces and reorganization energies in the exponential term of Eq. 1.19, is essential to optimize the balance between charge separation and charge recombination in a dyad. Even so, however, the lifetime of the charge separated state in dyads is usually too short to permit eventual charge accumulation and utilization (see below, however, for some purported exceptions). In order to overcome this limitation, a commonly used, biomimetic strategy has been that of increasing the supramolecular complexity of the system (from dyads to triads, tetrads, etc.) [33–36]. In such systems, multiple, sequential charge separation steps can take place and the expected exponential decrease of the electronic coupling V (Eq. 1.19) with distance [29, 37] can be exploited to slow down charge recombination. An example of such strategy is provided in Fig. 1.13, where the behavior of a simple porphyrin-fullerene dyad **D3** (Fig. 1.13a) is compared with that of a tetrad **T1** obtained by adding to the same dyad two further electron-donor units, namely zinc porphyrin and ferrocene [38]. The sequence of events taking place in **T1** is schematically shown in Fig. 1.13b.

Excitation of the free-base porphyrin (either by direct light absorption or following energy transfer from the zinc porphyrin) gives a primary charge separation process (144 ps), quite similar to that obtained in **D3**. In the tetrad, however, in competition with primary charge recombination (expected to take place, as in the dyad, in some 80 ns), a fast charge shift process takes place (400 ps) whereby the hole in the free-base porphyrin is filled by an electron from the zinc porphyrin. Now, in competition with secondary charge recombination (20 μ s), a further charge shift process takes place (5.9 ns) leading to the final charge separated state where the positive charge resides on the ferrocene unit. The fully charge-separated state $\text{Fc}^+ \text{-ZnP-H}_2\text{P-C}_{60}^-$ so obtained has a remarkable lifetime of 0.34 s, with a gain factor $> 10^6$ relative to the corresponding dyad system [38]. The key to this result is evident from the reaction scheme, namely, the strong (actually, exponential) decrease in the charge recombination rates, as the distance between the charges increases going from the dyad, to the triad, and finally to the tetrad. It is important to realize, however, that the remarkable elongation in lifetime achieved by the strategy of stepwise charge separation is obtained at the expenses of the energy of the CS state, and thus of the amount of light energy converted in redox potential. Therefore, in the design of artificial charge separating systems an appropriate balance has to be sought between the lifetime and the energy of the final charge separated state.

A sharply different strategy has been advocated by Fukuzumi [39] claiming that long-lived charge separation can be obtained even in very short dyads, provided that (i) the reorganization energy is very small, (ii) the charge separated state has high energy, and (iii) no locally excited triplet states of donor and acceptor are energetically accessible from the charge separated state. As an example, the dyad **D4** (Fig. 1.14), where the acridinium unit acts as a photoexcitable acceptor and the mesityl group as the donor, was reported to have an extremely long-lived electron

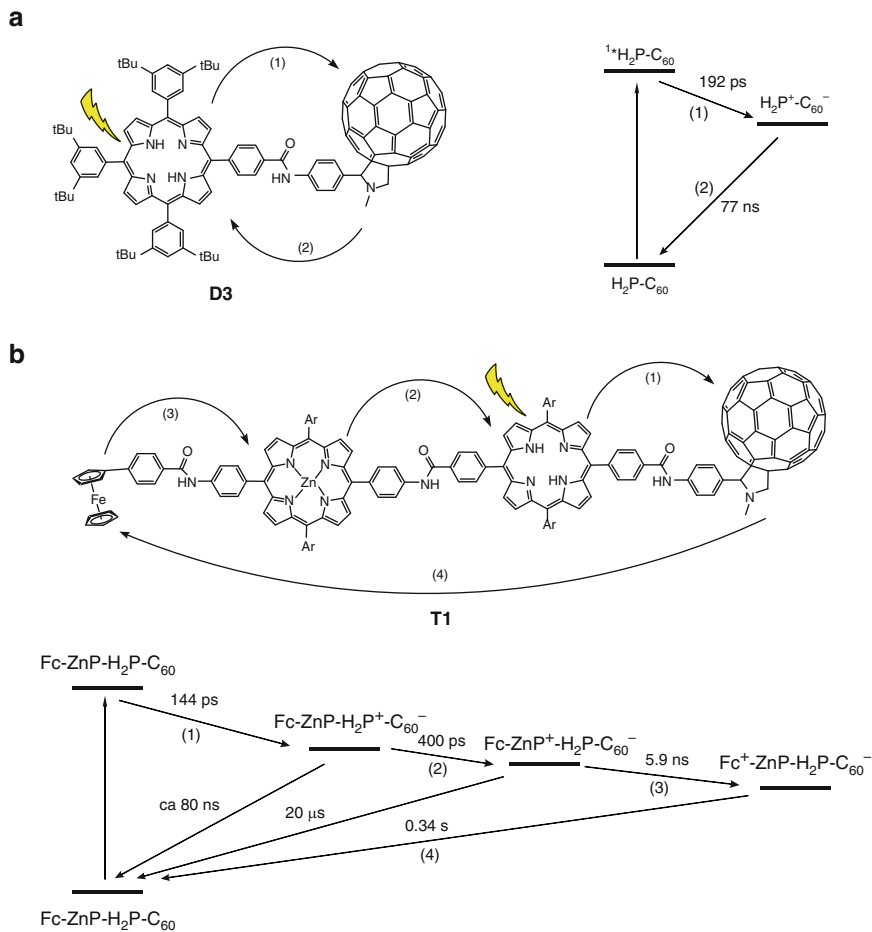
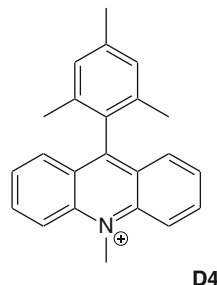


Fig. 1.13 Structure and photophysical behavior of (a) a porphyrin-fullerene dyad **D3** and (b) a ferrocene-zinc porphyrin-porphyrin-fullerene tetrad **T1**

Fig. 1.14 Molecular structure of the Acr^+ -Mes structure of the Acr^+ -Mes dyad **D4** described by Fukuzumi and coworkers



isomers). In the DQ-Ru-PTZ₂ pseudo-triad **T2** [42] the sensitizer is a tris (bipyridine) complex (Ru), the acceptor is a cyclo-quaternarized 2,2'-bipyridine (DQ) and the donor a phenothiazine (PTZ). In this system, photoinduced electron transfer from the sensitizer to the acceptor (ca 1 ns) is followed by fast hole transfer to the donor, with formation of a fully charge separated state that lives for 100–300 ns (dichloroethane, room temperature). In the MV-Ru-TAA triad **T3** [44d] the sensitizer is a bis(terpyridine) complex (Ru), the acceptor a methylviologen (MV), and the donor is a triarylamine (TAA). Here again, primary electron transfer to the acceptor (15 ns) is followed by fast hole transfer to the donor with formation of a fully charge separated state that lives for 27 ns (butyronitrile, 150 K, required for a manageable sensitizer excited-state lifetime).

All the examples of charge separating systems described so far have the sensitizer, donor, and acceptor units connected by organic covalent linkages. Though providing chemical robustness, the use of covalent organic techniques is often plagued by long synthetic routines and low yields. Inspired by the natural systems, where the cofactors are held in their positions by weak non-covalent interactions, some attempts have been made to obtain charge separating systems by spontaneous self-assembling of molecular components.

For such intrinsically non-symmetric systems, the problem is not obvious as it requires molecular recognition between the subunits to be assembled. In the example shown in Fig. 1.16, [47] the molecular building units designed to that purpose are: (i) an aluminium porphyrin (AlMPyP) as the central photoexcitable sensitizer, (ii) a naphthalenediimide (NDI) as electron acceptor unit, and (iii) a ruthenium porphyrin (RuP) as electron donor unit. The self-assembling ability is implemented by introduction of a carboxylic function (with great affinity for Al coordination) on the naphthalenediimide unit and of a pyridyl appended ligand (with strong affinity for Ru coordination) on the aluminium porphyrin. In fact, a single three-component adduct **T4**, NDI-AlMPyP-RuP, quantitatively self-assembles from a 1: 1: 1 mixture of the three starting units in dichloromethane. As demonstrated by ultrafast spectroscopy, excitation of the aluminium porphyrin is followed by stepwise electron (3 ps) and hole transfer (35 ps), leading to a charge separated state with reduced acceptor and oxidized donor (NDI⁻-AlMPyP-RuP⁺), with a lifetime in the few nanoseconds range [47].

The few examples shown above are meant to illustrate the main principles that underlie the design of artificial systems for charge separation. Implementing such strategies, with an appropriate choice of molecular components and supramolecular architecture, a variety of molecular devices featuring efficient and long-lived photoinduced charge separation have been produced in the last decades.

1.3.3 Antenna Systems

In natural photosynthesis, the antenna units are large arrays of chromophores that play the role of efficiently absorbing the incoming photons and to convey, by means

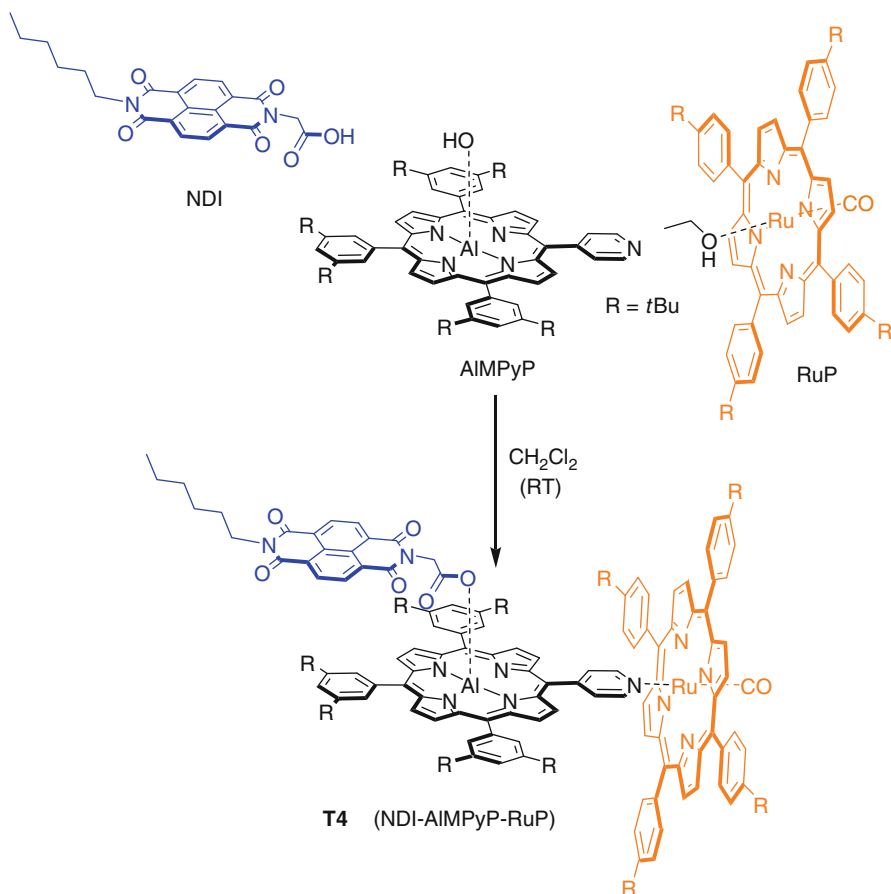


Fig. 1.16 Schematic representation of the self assembling process to obtain triad **T4**

of multiple energy transfer steps, the absorbed energy to the reaction centers (or photosystems) where charge separation takes place. Although in artificial photosynthetic systems the two functions, light absorption and charge separation, might not necessarily have to be as drastically distinguished as in Nature (see Sect. 1.2), substantial efforts have been devoted in recent years to the design and development of bioinspired artificial antenna systems.

Because of their similarity to the natural chlorophyll pigments, porphyrins have played the major role as chromophores for the construction of artificial antenna systems [48–52]. Other chromophores, such as, e.g., bodipy and perylene bisimides have been also frequently used, however. Out of the vast literature on this subject, [53] a few examples will be chosen so as to illustrate architecture strategies and functions.

A very interesting series of multichromophoric arrays has been developed and studied by Osuka and coworkers, based on zinc porphyrins directly linked in the

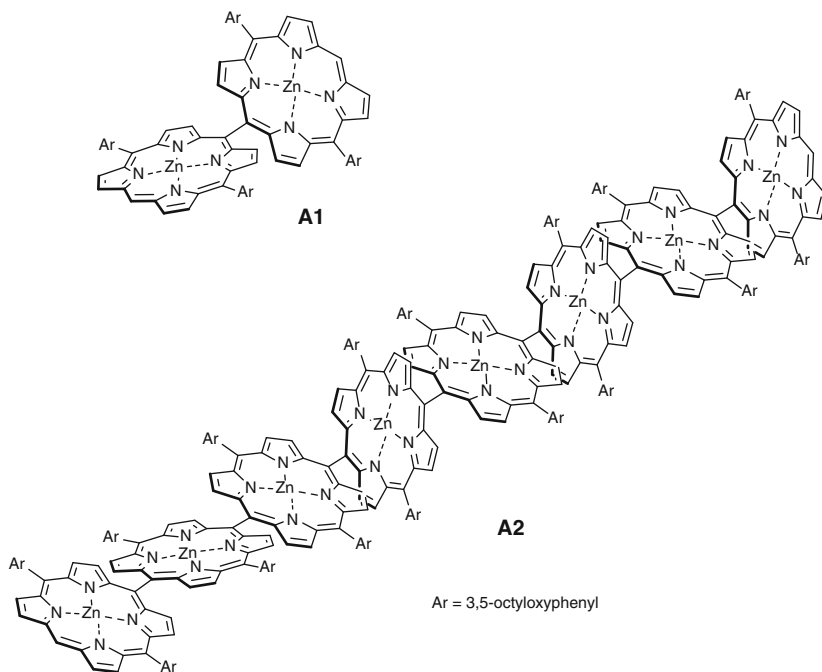


Fig. 1.17 Examples of the family of *meso-meso* linked linear porphyrin oligomers developed by Osuka and coworkers: dimer **A1** and octamer **A2**

meso positions via Ag-promoted coupling. Linear oligomers going from a simple dimer (**A1**) to tetramer, octamer (**A2**, Fig. 1.17), etc., up to a 128-mer of ca 106 nm (!) were obtained and studied [54]. In these systems, the orthogonality of the porphyrin rings imposed by steric hindrance prevents extensive π conjugation. However, the arrays exhibit dipole exciton coupling, with an exciton delocalization length (coherent length) extending over ca 4 adjacent porphyrin units. This favors fast singlet electronic energy transfer along the arrays (2.5–108 ps for arrays with $n = 2$ –25 units), as measured by time-resolved fluorescence in a series of linear arrays of the type shown in Fig. 1.17 in which a terminal energy acceptor unit (5,15-bisphenylethynylated porphyrin) is added to the array [55]. Inspired by the cylindrical shape of the bacterial photosynthetic antennas (Sect. 1.2.1), a series of related porphyrin arrays with cyclic structures was synthesized by connecting *meso-meso* linked dimers or tetramers via 1,3-phenylene bridges (**A3** and **A4**, respectively, Fig. 1.18) [52]. In these arrays, the excited state is considered to be delocalized over the *meso-meso* linked dimeric or tetrameric linear porphyrin subunit, and a Forster-type model can be used to interpret the fast electronic energy transfer rates (3.6 ps for **A3**, 35 ps for **A4**) observed in these cyclic systems [56].

Aside from directly linked systems, other families of arrays can be obtained by linking the individual porphyrin chromophores by means of organic bridging groups, usually in the *meso* positions. With ethyne or butadiyne as bridging groups,